THE ASTRONOMICAL JOURNAL, 121:2775–2780, 2001 May
© 2001. The American Astronomical Society. All rights reserved. Printed in U.S.A.

THE DISCOVERY OF CIRCUMSTELLAR ARCS AROUND TWO BIPOLAR PROTO–PLANETARY NEBULAE[1]

BRUCE J. HRIVNAK,[2] SUN KWOK,[3,4] AND KATE Y. L. SU[2,3]
Received 2000 November 13; accepted 2001 January 18

ABSTRACT

Circumstellar arcs have been discovered using the *Hubble Space Telescope* in two proto–planetary nebulae (PPNs), IRAS 16594−4656, and IRAS 20028+3910. This raises to five the number of PPNs in which such arcs have been detected and suggests that they are not rare and may even be common features. All five of these PPNs display a bipolar morphology, but this correlation may be the result of a selection effect in which deeper images are taken of bipolar PPNs in which the central star is obscured. Two pairs of oppositely directed "searchlight beams" are seen in IRAS 20028+3910, similar to those seen in AFGL 2688 and IRAS 17150−3224. The presence of circular arcs and rings in PPNs and planetary nebulae with a variety of viewing orientations implies that they are illuminated portions of spherical shells viewed in scattered light. This suggests that the mass-loss process is spherically symmetric over most of the lifetime of the progenitor asymptotic giant branch (AGB) star, and the transition to a bipolar morphology occurs over a short period at the end of the AGB evolution.

Key words: circumstellar matter — planetary nebulae: general — stars: AGB and post-AGB

1. INTRODUCTION

One of the most unexpected discoveries of the *Hubble Space Telescope* (*HST*) observations of planetary nebulae (PNs) is the revelation of concentric rings in the nebulae. As of mid-2000, circumstellar rings have been found in three planetary nebulae (NGC 7027, Bond 2000; NGC 6543, Balick, Wilson, & Hajian 2001; Bond 2000, Terzian & Hajian 2000; Hb 5, Terzian & Hajian 2000). Even though some of these nebulae have bipolar shapes, the rings are remarkably circular. The detection of similar circumstellar arcs and rings in proto–planetary nebulae (PPNs) (AFGL 2688, Sahai et al. 1998; IRAS 17150−3224, Kwok, Su, & Hrivnak 1998; IRAS 17441−2411, Su et al. 1998) and in the carbon star IRC+10216 (Mauron & Huggins 1999) suggests that they originate from the remnants of the circumstellar envelopes of the asymptotic giant branch (AGB) progenitors. If these arcs and rings are indeed common, they will have important implications for our understanding of mass loss on the AGB.

The study of these arcs and rings can also provide valuable insights into the shaping of PNs. PNs are known to have diverse morphologies, ranging from round to elliptical to bipolar shapes. Although the interacting stellar winds model has gone a long way toward explaining how the AGB winds are compressed into the shell-like structures of PNs, the exact mechanism responsible for the diverse morphologies observed in PNs is still not well understood (see Kastner, Soker, & Rappaport 2000). The simultaneous presence of the circular arcs and rings in PNs and PPNs with bipolar nebulosities therefore provides strong observational constraints on how and when the shaping occurs.

One of the first steps toward this goal is to establish that such circumstellar arcs and rings are in fact common. In this paper we report the discovery of two additional PPNs with circumstellar arcs. The state of our present knowledge of arcs and rings around post-AGB objects is then summarized, and some conclusions are drawn about the mass-loss process on the AGB.

2. *HST* IMAGES

Imaging of several PPNs candidates was carried out as part of the *HST* guest observing program 8210 (principal investigator, B. Hrivnak). The Wide Field Planetary Camera 2 (WFPC2) was used in the Planetary Camera mode, with the wide-band filter F814W ($\langle\lambda\rangle = 804$ nm, $\Delta\lambda = 154$ nm). Circumstellar arcs are seen in two of the objects, IRAS 16594−4656 and IRAS 20028+3910. These two were observed on 1999 June 28 and 1999 May 28, respectively. Two or three long observations were obtained in a dithered pattern for each, totaling 1000 and 1800 s, respectively. These were combined to remove cosmic rays and were "drizzled" (Fruchter & Hook 1997) to improve the spatial resolution, which is 0.″10 for each.

Images of the two nebulae are presented in Figures 1 and 2. In both images, intensity levels are adjusted to show the faint outer arcs, with the result that the bright central parts of the nebulae appear saturated. Both nebulae display bipolar morphologies, but with very different appearances, presumably because of their different orientations and the different densities of their circumstellar envelopes. *HST* images of IRAS 16594−4656 (Water Lilly Nebula) that clearly show the central star and the bipolar lobes are displayed and discussed by Hrivnak, Kwok, & Su (1999). Similarly, the inner regions of IRAS 20028+3910 can be seen in the shorter exposure images of Ueta, Meixner, & Bobrowsky (2000); however, no central star is seen in this object.

The arc structures displayed are enhanced slightly by the application of an unsharp filter to the images. In IRAS 16594−4656, at least four arcs are seen at different radii

[1] This work was based on observations with the NASA/ESA *Hubble Space Telescope* obtained at the Space Telescope Institute, which is operated by the Association of Universities for Research in Astronomy, Inc., under NASA contract NAS 5-26555.

[2] Department of Physics and Astronomy, Valparaiso University, Valparaiso, IN 46383-6493; bruce.hrivnak@valpo.edu, ksu@kate.su.valpo.edu.

[3] Department of Physics and Astronomy, University of Calgary, 2500 University Drive, Science B Building, Room 605, Calgary AB T2N 1N4 Canada; kwok@iras.ucalgary.ca.

[4] Canada Council Killam Fellow.

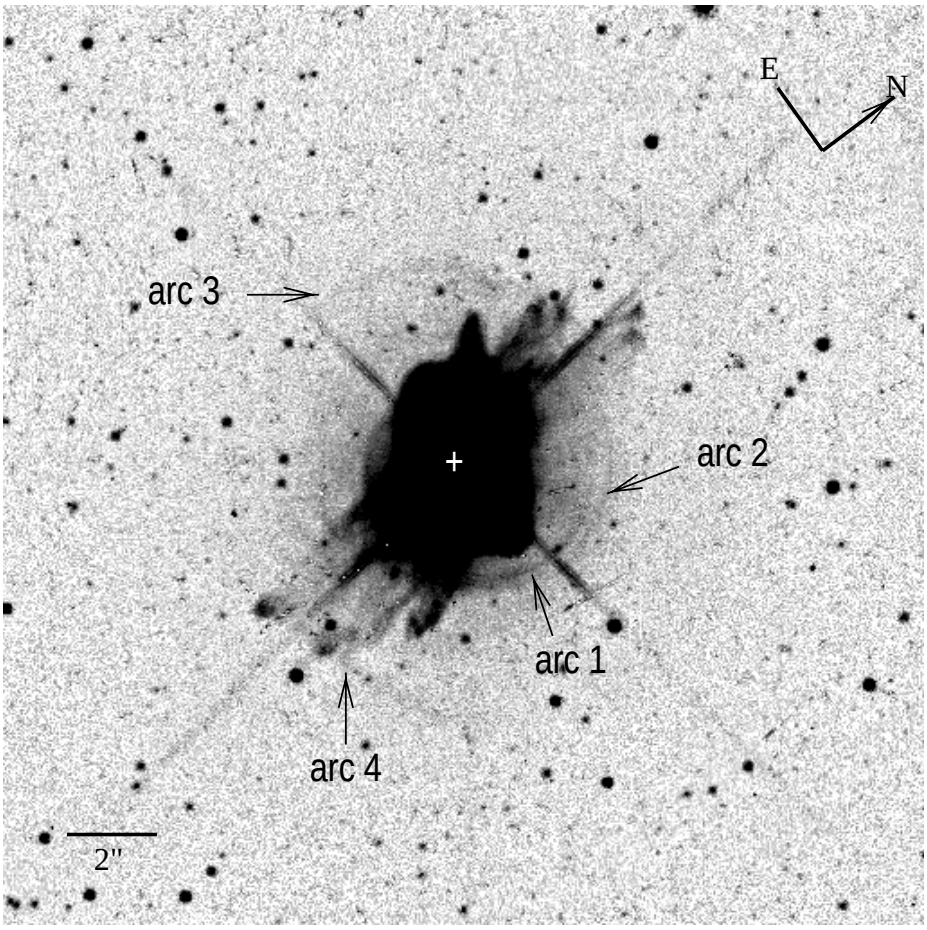


FIG. 1.—*HST* WFPC2 image of IRAS 16594−4656 with the F814W filter, after application of an unsharp mask, showing the center of the arcs (*plus sign*), also the location of the visible star. The intensities are displayed on a logarithmic scale to bring out the faint arcs. The central regions are saturated on this display. Four of the arcs are labeled, but possibly more are present.

from the central star. The arcs are concentric, centered on the visible central star. Arc 1 is located 3.″36 from the central star, and the separation between successive arcs is 0.″48, 1.″43, and 0.″80, as measured in the outward direction. Arc 1 can be seen continuously for about 180° around the central star, with variations in brightness. Arc 2 is fainter, but can be seen to extend over the same angular region. Arc 3 can be seen to trace out about 90° in the sky, and arc 4, about 45°. There are suggestions of several more arcs between arcs 2 and 3, but they are too faint to qualify as definite detections. Arcs 1, 2, and 4 are seen on the southwest side of the nebulae, the side with the brighter lobe, while arc 3 is seen on the side of the fainter lobe. In fact, one can look back at the shorter exposure (480 s) image by Hrivnak et al. (1999) and faintly see parts of all four of these arcs, although they were not recognized at that time.

A radial cut through a well-defined section of arc 1 indicates a deconvolved thickness of 0.″23. Based on this radial cut across arcs 1 and 2, we estimate the brightness ratio between the arcs and the continuum to be about 1.1 for both arcs. If the brightness is proportional to density, these values suggest that the density enhancements in the arcs are at least 10%. If we include the consideration of projection effects in which the observed arc intensity is averaged over intershell regions along the line of sight, the actual density enhancement is likely to be larger than 10%.

Three opposite pairs of arcs of differing brightness are seen in the image of IRAS 20028+3910. These arcs are much smaller in angular extent than are those of IRAS 16594−4656, and subtend angles of $\lesssim$45°. They are all aligned approximately along the long axis of the teardrop-shaped bright region of the southeastern lobe, but not exactly along this axis. One group of three is just beyond the southeastern end of the bright lobe and the other group lies by itself northwest of the bright lobe. In fact, the expected second, northwestern lobe of the nebula is not seen; presumably it is obscured by a wide opaque disk that covers this lobe but not the innermost arc. On the northwestern side, arc 1 is clearly visible, arc 2 is barely visible, and arc 3 is perhaps barely visible. On the southeastern side, arc 1 is visible at the end of the lobe, and arcs 2 and 3 each appear as blobs of light with a faint extension of an arc. These arcs can also be seen in linear cuts of the intensity profile in the directions of the arcs, as shown in Figure 3. There may even be an additional blob of light beyond arc 3 on the southeastern side, approximately colinear with the blobs of arcs 2 and 3. Although these arcs are small in size, they appear to be consistent with the hypothesis that they are also concentric about a point that we assume to be the location of the central star. This point is marked on Figure 2 and is at the following position: R.A. (J2000.0) = $20^{h}04^{m}35^{s}.96$ and decl. (J2000.0) = +39°18′43.″8. The inner arc has a radius of 1.″15, and the successive arcs are separated by 0.″25 and 0.″32, as measured in the outward direction.

One can also see a pair of faint searchlight beams in the image of IRAS 20028+3910, which appear to illuminate the

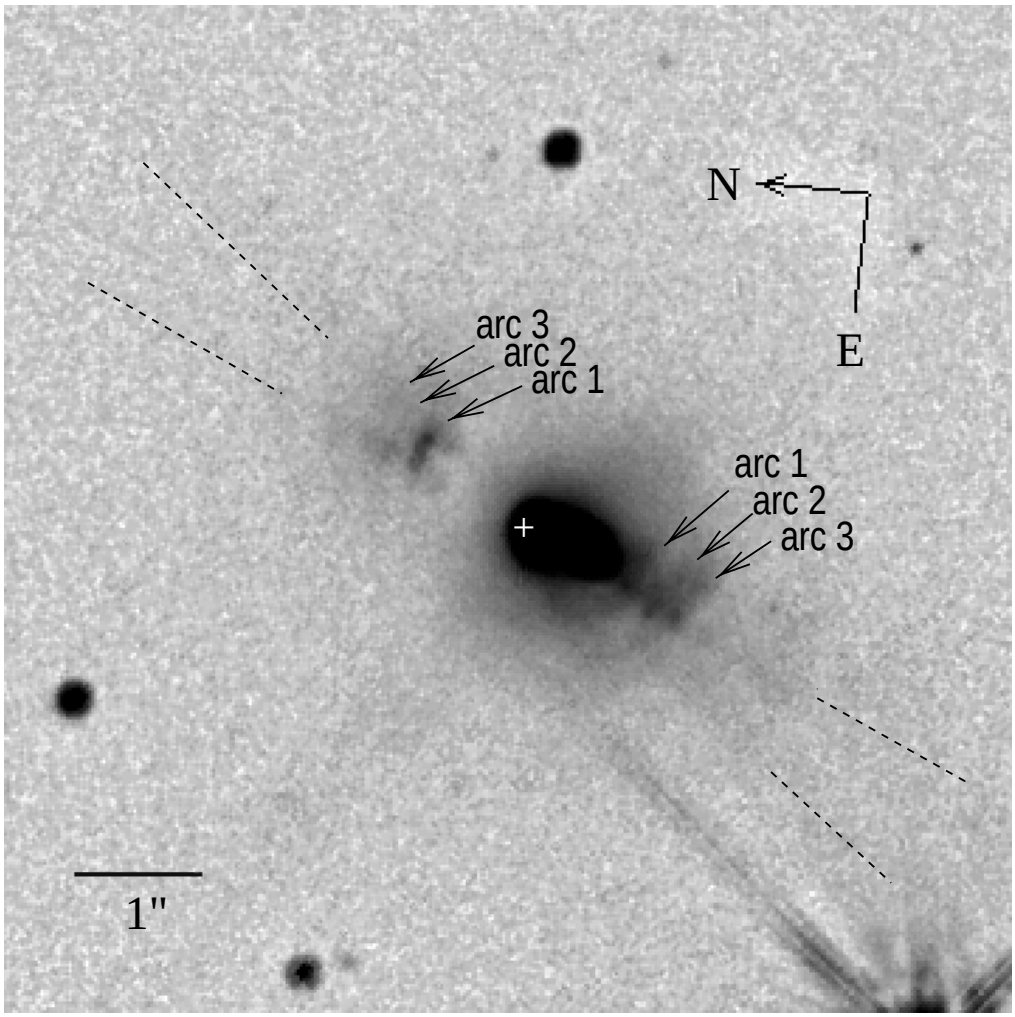


FIG. 2.—Similar to Fig. 1, but an image of IRAS 20028+3910. The locations of the two searchlight beams are indicated by dashed lines extending outward from the beams. (The streak arising from the lower right in the image of IRAS 20028+3910 is part of the diffraction spikes of a nearby bright star.)

arcs. The angular separation of the two beams is $14° \pm 1°$. Because of the diffuseness and faintness of the beams, the location of their crossing point is not well determined, but to within these uncertainties it is consistent with the center of the arcs, which we assume to be the location of the central star. The bright southeastern lobe is not quite aligned with the searchlight beams but is offset by a small angle.

3. DISCUSSION

The classification of these two objects as PPNs is based on their spectral energy distributions (SEDs) and optical spectra. PPNs are characterized observationally by a large infrared excess due to cool dust with a color temperature of 150–300 K, by an expanding molecular envelope, and by a central star with the spectral classification of a B–K supergiant (Kwok 1993). The optical counterparts of both IRAS 16594−4656 and IRAS 20028+3910 were identified as a result of our ground-based follow-up of cool *IRAS* sources. Both display double-peaked SEDs, with the peak in the mid-infrared much brighter than the peak in the visible near-infrared (see Hrivnak et al. 1999 for the SED of IRAS 16594−4656). The temperature of the dust component in the two objects is 170–180 K. The optical spectrum of IRAS 16594−4656 shows Hα, Hβ, and weak [O I] lines in emission (García-Lario et al. 1999), with a spectral type of B7 (Van de Steene, Wood, & van Hoof 2000). We classify it as a PPN; it does not show the collisionally excited forbidden lines we associate with a PN. We recently obtained low-resolution optical spectra of IRAS 20028+3910; these indicate a mid- to late-F spectral type, although they are of low signal-to-noise ratio. Thus we also classify IRAS 20028+3910 as a PPN. Both PPNs also possess expanding molecular CO envelopes (Loup et al. 1993).

The detection of concentric arcs in these two nebulae makes a total of five PPNs found to show such features. The best example, AFGL 2688, shows at least 20 arcs; however, these arcs do not seem to be exactly concentric, but appear to intersect in some cases. In IRAS 17150−3224, eight arcs are seen; these are concentric and relatively uniform in spacing, with an average separation of 0.″51 between the inner five, and a somewhat larger spacing between the outer ones (Kwok et al. 1998). In IRAS 17441−2441, at least two arcs are seen, with hints of others that might be confirmed in deeper images (Su et al. 1998). As mentioned earlier, concentric rings have recently been seen in the *HST* images of three PNs (NGC 7027, Hb 5, and NGC 6543). For NGC 6543, the arcs are seen in emission (Balick et al. 2001), rather than in scattered light as is the case for the arcs in the PPNs. Thus the arcs appear to be regions of enhanced dust and

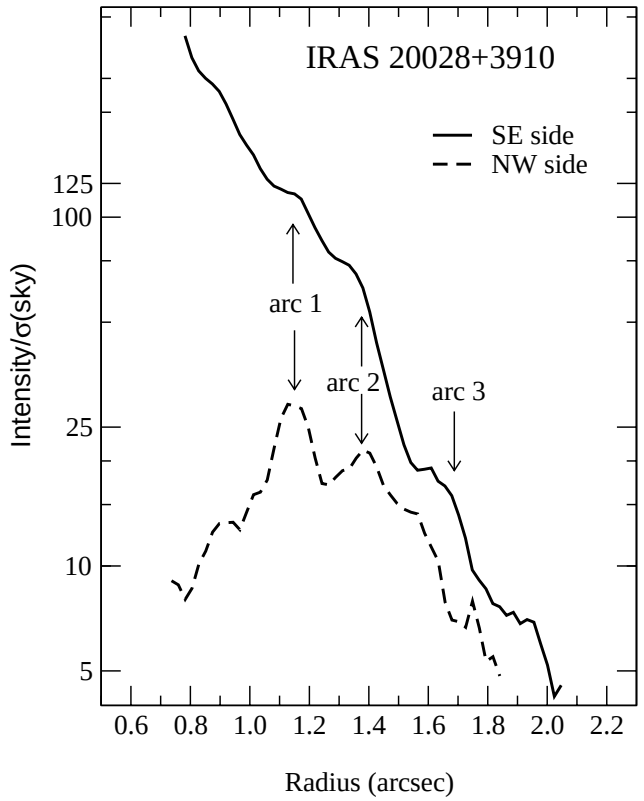


FIG. 3.—Approximately radial cuts in the intensity profile of the outer regions of IRAS 20028 + 3910, showing the locations of the arcs.

gas. The images of these three PNs have been retrieved from the *HST* archive and the arc separations measured. The observational properties of the arcs in these eight objects are summarized in Table 1.

The small number of PNs in which these rings and arcs have been detected should not necessarily be taken as an indication of the rareness of this phenomenon. Since the arcs are sharp and faint when compared with the bright inner structures seen in these PNs, they are hard to see without sensitive, high angular resolution imaging, such as is available with the *HST*. The rate of detection is much higher in PPNs, but these are all cases in which either the lobes are relatively large and bright with no central star visible (AFGL 2688, IRAS 17150−3224, and IRAS 17441−2411) or deep observations were intentionally made with the *HST* to search for such arcs (IRAS 16594−4656 and IRAS 20028 + 3910).

The presently available high-resolution (*HST*) imaging data on PPNs contain a number of biases that make it difficult to quantify how common such arcs may be in PPNs. In our recent *HST* imaging study, we also took long exposures (total times of 1000–1800 s) of four other PPN candidates in which we did not detect arcs. These are all bipolar, two seen approximately edge-on and two at an intermediate orientation. Thus in our small sample of relatively deep observations of eight PPNs (IRAS 17150−3224, 17441−2411, 16594−4656, and 20028 + 3910 and the four candidates mentioned above), all selected because they appeared to be extended and asymmetric in ground-based observations, arcs were detected in four, or 50%. However, this percentage could represent a lower limit for this sample. In the four cases without detected arcs, the PPNs seem to be much farther away than these two new cases with detected arcs, as judged by the fact that the observed flux densities of these four were all more than a factor of 3 lower, even when corrected for interstellar extinction (Su, Hrivnak, & Kwok 2001). Since the arcs in these two objects are visible but faint, it would be even more difficult to detect arcs in more distant objects since they would be even fainter and smaller, at or below our ability to resolve them. The other sample of PPNs available to investigate the frequency of arcs is the *HST* snapshot survey by Ueta et al. (2000). However, this survey was not designed to go as deep on faint objects, and thus was not well-suited to find faint arcs. They did see the previously detected arcs in IRAS 17150−3224 and 17441−2411 but not the newly detected arcs in IRAS 20028 + 3910. The objects in their survey often contained a bright central star, and although they did achieve a high dynamic range by obtaining images at varying exposure times they nevertheless did not go very deep. Even among the fainter objects in their sample only one was observed with a total exposure time longer than 700 s per filter, and that one we also observed even longer without detecting arcs. PPNs in which the central star appears bright may be the consequence of looking more nearly pole-on at a bipolar structure. Detecting arcs and rings in a bipolar PPN viewed nearly pole-on would be extremely difficult. The projected rings far from the star would receive little light because of obstruction by an equatorial region of enhanced

TABLE 1

SUMMARY OF ARCS AND RINGS AROUND PPNs, PNs, AND AGB STARS

Object	Type	Rings	Angular Spacing (arcsec)	V_{exp} (km s^{-1})	Ref.	Time Interval (yr kpc^{-1})	Comments
AFGL 2688.....	PPN	>20	0.3–1.1	19	1	75–275	Some intersecting
IRAS 16594−4656.....	PPN	>4	0.5–1.4	16	1	150–410	Concentric
IRAS 17150−3224.....	PPN	8	0.5–0.7	15	2	160–220	Concentric
IRAS 17441−2411.....	PPN	2	0.6	15	2	190	Concentric
IRAS 20028+3910.....	PPN	3	0.25–0.33	16	1	75–100	Possibly concentric
NGC 7027	PN	9	2.2–5.8	16	1	650–1700	Not concentric, some intersecting[a]
Hb 5.....	PN	6	0.6–1.3	15[b]	...	190–410	Concentric[a]
NGC 6543	PN	11	2.2–3.8	15[b]	...	700–1200	Concentric[a]
IRC+10216	AGB	>6	5–20	15	1	1600–6400[c]	Not concentric[a]

[a] Based on analysis of archival *HST* images.
[b] Assumed a typical value.
[c] For a distance of 120 pc (Loup et al. 1993), this translates into a time interval of 200–800 yr.
REFERENCES.—References for the velocity measurements are (1) Loup et al. 1993; (2) Hu et al. 1994.

density (that leads to the bipolar structure). The visibility of arcs or rings along the direction of the lobes would be greatly reduced by dilution from the light of the lobes. This is probably why arcs have been detected only in PPNs that have an edge-on or intermediate orientation. Thus, although the number of detections is small, it appears that circumstellar arcs and rings may be a common and perhaps even a universal phenomenon among PNs and PPNs and may commonly form during the end of the AGB mass-loss phase.

Among these objects with arcs, AFGL 2688, IRAS 17150−3224, IRAS 17441−2441, and Hb 5 are nearly edge-on bipolar systems, whereas NGC 7027 and the two new PPNs with arcs reported here are oriented at intermediate viewing angles. This suggests that these arcs are not part of two-dimensional circular features on the plane of the sky but *projections of limb-brightened spherical shells*. The fact that such rings are also seen in the AGB star IRC+10216 (Mauron & Huggins 1999), which is known from molecular line observations to have a spherical envelope, also supports this conclusion. If the rings and arcs observed in PNs, PPNs, and IRC+10216 are all part of the same phenomenon, then one can draw the conclusion that mass loss in the AGB progenitors of these PNs and PPNs must have been spherically symmetric.

The observed variation in brightness of the arcs with angle is probably the result of illumination. We note that in nearly edge-on systems (e.g., IRAS 17150−3224), the arcs are brightest in the lobes where the starlight escapes. In the case of IRAS 16594−4656, which has an intermediate orientation (Hrivnak et al. 1999), the angular brightness distribution of the arcs is more uniform.

If these rings are part of the AGB mass-loss process, what is their physical origin? The most obvious interpretation would be that they represent periods of enhanced mass loss. As can be seen from Table 1, their separations translate to timescales of many hundred to a thousand years. As has been noted previously by others, these timescales are much longer than the observed pulsational periods of AGB stars ($\sim$1 yr), but much shorter than the timescale of thermal pulses (10^4–10^5 yr). One possibility is that these shells are the result of instabilities. For example, Deguchi (1997) has suggested that the instability in the gas-dust coupling in a radiation pressure–driven outflow can create density waves that resemble discrete shells. An alternative source of cyclical perturbation would be a binary companion. Harpaz, Rappaport, & Soker (1997) suggest a model in which a periodic incursion by a stellar or planetary companion in an eccentric orbit causes a periodic decrease in an isotropic mass outflow, instead causing mass to be diverted toward the companion during the perihelion passage. A different mechanism, which also requires a binary companion, has been put forward by Mastrodemos & Morris (1999). In their model, the interaction of the companion star on the mass outflow produces expanding spiral shocks. Such density structures can cover most of the solid angle around the star and can be observed from any orientation. Another process that could operate on 10^2 yr timescales is the magnetic cycle of AGB stars (Soker 2000) The increased number of cool stellar spots during cycle maxima can enhance dust formation and therefore increase the mass-loss rate. If the cool spots are distributed uniformly over the stellar surface, spherical shells can be formed by the increased magnetic activities during cycle maxima. If this is indeed the mechanism, then the observations of circumstellar arcs will provide useful information on magnetic activities in late-type stars.

Regardless of the mechanism that creates the circumstellar arcs, our results also raise the question of the survival of the arcs over timescales of more than 10^4 yr. It is now commonly accepted that during the transition from the AGB to the PN phase, the star initiates a fast outflow that shapes the spherical circumstellar envelope into a bipolar form. How can the spherical shells remain intact during this transition? In a leading model that produces the bipolar morphology, the angular distribution of the AGB wind material causes the fast-slow wind interaction to be channeled into volumes within a limited solid angle, creating a cavity as the gas is swept up (Frank 1999). Alternatively, the cavity could be carved out by a collimated fast outflow (Sahai & Trauger 1998). In either case, while any arc structure within the cavity would have been destroyed, the shells outside the cavity would remain and the arcs that are seen would represent projections of the undisturbed spherical shells.

All five PPNs that show the circumstellar arcs also display a clear bipolar morphology. This might suggest some common mechanism that produces both phenomena. However, this apparent correlation may simply be an observational selection effect. PPNs with bright central stars tend to be observed with shorter exposures to minimize saturation effects, while those in which the central star is partially or completely obscured tend to be observed with longer exposure times to bring out the fainter lobes and halo. Thus one must await a more systematic study of deep images of PPNs with various apparent morphologies to determine whether there is a correlation between the presence of circumstellar arcs and a bipolar morphology. One should keep in mind, however, that all PPNs may have a basic bipolar structure, with the differences in morphology due to differences in the viewing orientation and differences in the optical depth of the circumstellar matter (Hrivnak, Kwok, & Su 2000).

The radial "searchlight beam" appearance seen in IRAS 20028+3910 has also been seen in AFGL 2688 and IRAS 17150−3224, making a total of three bipolar PPNs known thus far to display this phenomenon. The beams may be caused by light reflecting off the cavity walls, in which case the angular separation between the beams can be interpreted as the opening angle of the conical shape at the base of the cavities. Another interpretation advanced for the Egg Nebula is that the beams represent light that escapes through annular holes carved out by a high-velocity outflow (Sahai et al. 1998). In either model the lack of alignment between the searchlight beams and the lobe in IRAS 20028+3910, in contrast to the alignment seen in the other two, is hard to understand and we do not have a satisfactory explanation for it.

The detection of these searchlight beams would be favored in bipolar systems that are being viewed close to edge-on, and would be difficult to see in nearly pole-on systems.

4. SUMMARY AND CONCLUSIONS

Deep *HST* images have been used to discover concentric arcs in two additional PPNs, bringing the total to five PPNs and three PNs that show this phenomenon. These arcs and rings appear to be the illuminated portions of

spherical shells that likely formed by density enhancements of the circumstellar mass ejected during the proceeding AGB phase. The persistence of these rings from the AGB to the PPN to the PN phase suggests that most parts of the AGB envelope are not affected during this transition and that the shaping of PNs can be accomplished by wind interactions over a small solid angle.

Since the present sample includes only objects with strong circumstellar dust emissions and deep, high-resolution images, it is possible that this sample represents only the "tip of the iceberg" of this phenomenon. The available evidence suggests that circumstellar rings may be a common phenomenon in AGB envelopes and post-AGB nebulae. A deep, high-resolution imaging survey is needed to quantify the universality of circumstellar arcs and rings and the roles they play in the last stages of stellar evolution.

Support for this work was provided by NASA to B. J. H. through grant GO-08210.01-97A from the Space Telescope Science Institute, which is operated by the Association of Universities for Research in Astronomy, Inc., under NASA contract NAG 5-26555, and by a grant to S. K. from the Natural Science and Engineering Research Council of Canada. B. J. H. acknowledges the support of a University Research Professorship from Valparaiso University and the hospitality of the Steward Observatory, where part of this research was carried out.

REFERENCES

Balick, B., Wilson, J., & Hajian, A. R. 2001, AJ, 121, 354
Bond, H. 2000, in ASP Conf. Ser. 199, Asymmetrical Planetary Nebulae II: From Origins to Microstructures, ed. J. H. Kastner, N. Soker, & S. Rappaport (San Francisco: ASP), 115
Deguchi, S. 1997, in IAU Symp. 180, Planetary Nebulae, ed. H. J. Habing & H. J. G. L. M. Lamers (Dordrecht: Kluwer), 151
Frank, A. 1999, NewA Rev., 43, 31
Fruchter, A. S., & Hook, R. N. 1997, Proc. SPIE, 3164, 120
García-Lario, P., Manchado, A., Ulla, A., & Manteiga, M. 1999, ApJ, 513, 941
Harpaz, A., Rappaport, S., & Soker, N. 1997, ApJ, 487, 809
Hrivnak, B. J., Kwok, S., & Su, K. Y. L. 1999, ApJ, 524, 849
———. 2000, in ASP Conf. Ser. 199, Asymmetrical Planetary Nebulae II: From Origins to Microstructures, ed. J. H. Kastner, N. Soker, & S. Rappaport (San Francisco: ASP), 155
Hu, J. Y., te Lintel Hekkert, P., Slijkhuis, S., Sahai, R., & Wood, P. R. 1994, A&AS, 103, 301
Kastner, J. H., Soker, N., & Rappaport, S. A., ed. 2000, ASP Conf. Ser. 199, Asymmetrical Planetary Nebulae II: From Origins to Microstructures (San Francisco: ASP).
Kwok, S. 1993, ARA&A, 31, 63
Kwok, S., Su, K. Y. L., & Hrivnak, B. J. 1998, ApJ, 501, L117
Loup, C., Forveille, T., Omont, A., & Paul, J. F. 1993, A&AS, 99, 291
Mastrodemos, N., & Morris, M. 1999, ApJ, 523, 357
Mauron, N., & Huggins, P. J. 1999, A&A, 349, 203
Sahai, R., & Trauger, J. T. 1998, AJ, 116, 1357
Sahai, R., et al. 1998, ApJ, 493, 301
Soker, N. 2000, MNRAS, 312, 217
Su, K. Y. L., Hrivnak, B. J., & Kwok, S. 2001, in preparation
Su, K. Y. L., Volk, K., Kwok, S., & Hrivnak, B. J. 1998, ApJ, 508, 744
Terzian, Y., & Hajian, A. R. 2000, in ASP Conf. Ser. 199, Asymmetrical Planetary Nebulae II: From Origins to Microstructures, ed. J. H. Kastner, N. Soker, & S. Rappaport (San Francisco: ASP), 33
Ueta, T., Meixner, M., & Bobrowsky, M. 2000, ApJ, 528, 861
Van de Steene, G. C., Wood, P. R., & van Hoof, P, A. M. 2000, in ASP Conf. Ser. 199, Asymmetrical Planetary Nebulae II: From Origins to Microstructures, ed. J. H. Kastner, N. Soker, & S. Rappaport (San Francisco: ASP), 191